A selective EP4 PGE_2 receptor agonist alleviates disease in a new mouse model of X-linked nephrogenic diabetes insipidus

Jian Hua Li,[1] Chung-Lin Chou,[2] Bo Li,[1] Oksana Gavrilova,[3] Christoph Eisner,[4] Jürgen Schnermann,[4] Stasia A. Anderson,[5] Chu-Xia Deng,[6] Mark A. Knepper,[2] and Jürgen Wess[1]

[1]Molecular Signaling Section, National Institute of Diabetes and Digestive and Kidney Diseases, [2]Laboratory of Kidney and Electrolyte Metabolism, National Heart, Lung, and Blood Institute, [3]Mouse Metabolic Core Facility and [4]Renal Function and Injury Section, National Institute of Diabetes and Digestive and Kidney Diseases, [5]Animal MRI/Imaging Core, National Heart, Lung, and Blood Institute, and [6]Mammalian Genetics Section, Genetics of Development and Diseases Branch, National Institute of Diabetes and Digestive and Kidney Diseases, NIH, Bethesda, Maryland, USA.

X-linked nephrogenic diabetes insipidus (XNDI) is a severe kidney disease caused by inactivating mutations in the V2 vasopressin receptor (V2R) gene that result in the loss of renal urine-concentrating ability. At present, no specific pharmacological therapy has been developed for XNDI, primarily due to the lack of suitable animal models. To develop what we believe to be the first viable animal model of XNDI, we generated mice in which the *V2R* gene could be conditionally deleted during adulthood by administration of 4-OH-tamoxifen. Radioligand-binding studies confirmed the lack of V2R-binding sites in kidneys following 4-OH-tamoxifen treatment, and further analysis indicated that upon V2R deletion, adult mice displayed all characteristic symptoms of XNDI, including polyuria, polydipsia, and resistance to the antidiuretic actions of vasopressin. Gene expression analysis suggested that activation of renal EP4 PGE_2 receptors might compensate for the lack of renal V2R activity in XNDI mice. Strikingly, both acute and chronic treatment of the mutant mice with a selective EP4 receptor agonist greatly reduced all major manifestations of XNDI, including changes in renal morphology. These physiological improvements were most likely due to a direct action on EP4 receptors expressed on collecting duct cells. These findings illustrate the usefulness of the newly generated V2R mutant mice for elucidating and testing new strategies for the potential treatment of humans with XNDI.

Introduction

In nephrogenic diabetes insipidus (NDI), the kidney is unable to conserve water despite normal or increased plasma levels of the antidiuretic hormone arginine vasopressin (AVP) (1–5). Most patients (>90%) with congenital NDI harbor inactivating mutations in the V2 vasopressin receptor (*V2R*) gene, which is located on the long arm of the X chromosome (2–7). This form of NDI, which is commonly referred to as X-linked NDI (XNDI), therefore almost exclusively manifests itself in males.

After its release into the bloodstream from the posterior pituitary gland, AVP binds to renal V2Rs, which are expressed in the principal cells of the renal collecting duct system (2–7). AVP binding to the V2R triggers the activation of the stimulatory G protein G_s, resulting in elevated intracellular cAMP levels which, through several intermediate steps, eventually promote the insertion of aquaporin-2 (AQP2) water channels into the luminal membrane of the principal cells (8). This mechanism allows for the passive movement of water from the tubule lumen into the kidney interstitium and eventually into the bloodstream. Moreover, prolonged V2R activity further promotes osmotic reabsorption of water from the tubule lumen by triggering increases in AQP2 and aquaporin-3 (AQP3) expression levels in renal collecting duct cells (9, 10).

At present, more than 200 different disease-causing V2R mutations have been identified (11). Loss of V2R function in XNDI patients interferes with water reabsorption in the renal collecting duct system, resulting in the production of large volumes (>30 ml/kg/d) of dilute urine (<250 mOsmol/kg) (polyuria) and excessive thirst (polydipsia). Hypernatremia and dehydration, which are among the most severe complications associated with XNDI, may cause chronic renal insufficiency as well as mental retardation, at least in a subgroup of XNDI patients (1, 2). Long-term complications include large dilatations of the urinary tract and bladder as well as kidney failure secondary to bilateral hydronephrosis (1, 2, 5). Newborns suffering from XNDI frequently show poor weight gain and an overall failure to thrive, sometimes complicated by convulsions or death due to hypertonic dehydration, especially if XNDI is not diagnosed early enough (1, 2).

Currently, no specific, highly effective pharmacological therapy has been developed for the treatment of XNDI (1–3), primarily due to the lack of suitable animal models. We previously created V2R-KO mice lacking functional V2Rs throughout development (12). However, mutant XNDI pups died within the first postnatal week due to massive dehydration (12).

We here report the generation of viable V2R mutant mice in which the *V2R* gene can be deleted in a conditional fashion in adult mice. Using this new mouse model, we demonstrate that a compound that selectively activates the EP4 PGE_2 receptor subtype (ONO-AE1-329 [ONO]; ref. 13) is highly effective in ameliorating all major manifestations of XNDI, including failure to concentrate urine, polyuria, and dilatation of the renal pelvis, most likely through a direct action on EP4 receptors expressed by kidney collecting duct cells. These findings should stimulate the development of a new generation of drugs useful for the treatment of human XNDI.

Conflict of interest: The authors have declared that no conflict of interest exists.
Citation for this article: *J. Clin. Invest.* **119**:3115–3126 (2009). doi:10.1172/JCI39680.

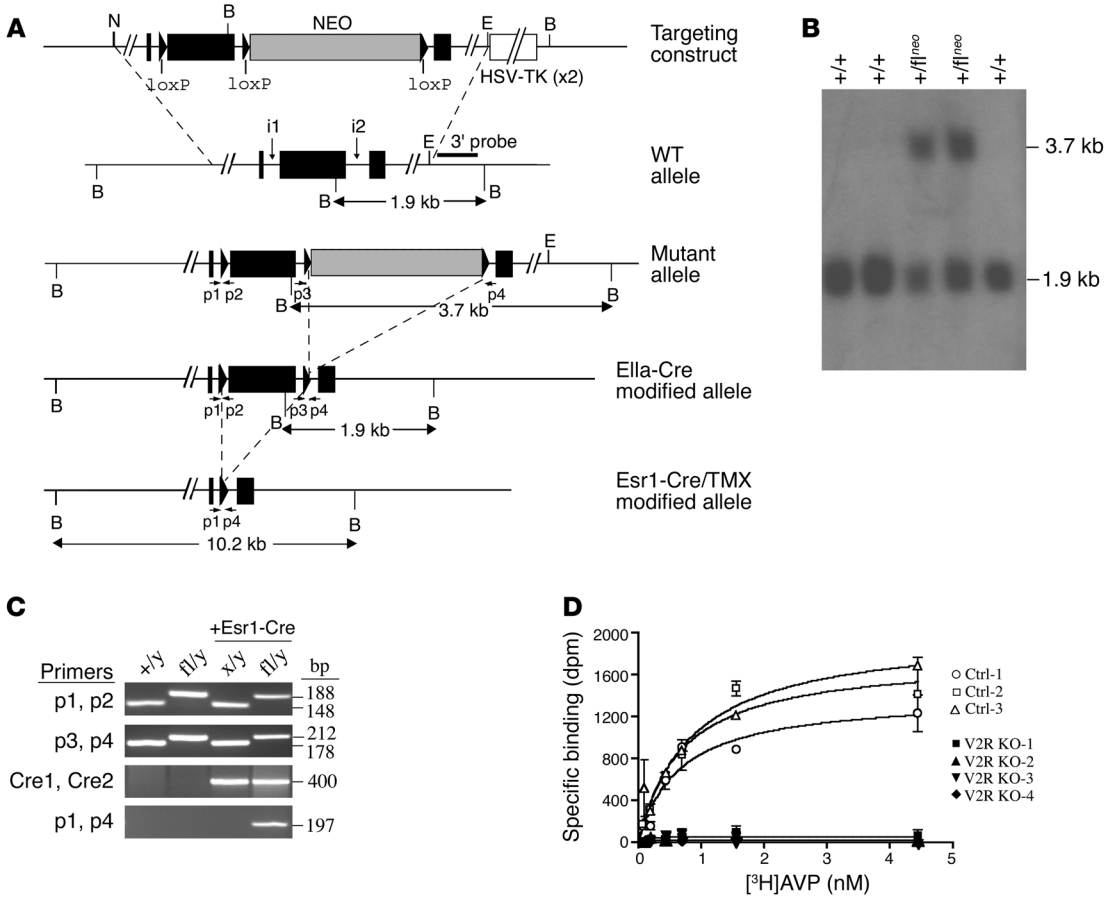

Figure 1

Targeting strategy for conditional disruption of the mouse *V2R* gene. (**A**) Structures of the targeting construct, the WT V2R locus, the recombined mutant allele, and the EIIa-Cre– and Esr1-Cre–modified V2R alleles. Note that the V2R coding sequence (represented by the 3 filled boxes) is disrupted by 2 short introns (i1 and i2). The positions of the PCR primers used for genotyping studies (p1–p4) are indicated (see Methods for details). B, BamHI; E, EcoRI; N, NotI. (**B**) Genotyping of female F2 mice to verify the proper integration of the targeting vector via Southern blot analysis. Genomic DNA prepared from tails of female F2 WT (+/+) or heterozygous V2R mutant mice (+/fl^{neo}) mice was digested with BamHI and subjected to Southern blot analysis using the 3′ probe (see **A**). The 1.9- and 3.7-kb bands represent the WT and the mutant V2R fl^{neo} alleles, respectively. (**C**) PCR analysis of genomic DNA prepared from kidneys of male mice of the indicated V2R genotypes. The location of PCR primers p1–p4 is indicated in **A**. Use of PCR primers p1 and p4 resulted in a 197-bp band only in the case of kidney DNA prepared from TMX-treated $V2R^{fl/y}$*Esr1-Cre* mice, indicative of Cre-mediated disruption of the *V2R* gene. (**D**) [^{3}H]-AVP–binding studies. [^{3}H]-AVP saturating binding studies were carried out with whole-kidney membrane homogenates prepared from 4 male TMX-treated $V2R^{fl/y}$*Esr1-Cre* mice (V2R-KO mice) and 3 control (Ctrl) littermates (TMX-treated $V2R^{fl/y}$ mice) (mouse age, 8 months; see Methods for details).

Results

Generation of conditional V2R-KO mice. The gene-targeting strategy used for generating an inducible mouse model of XNDI is shown in Figure 1A. Importantly, the targeting construct contained a *neo* selection cassette, flanked by 2 loxP sites, that was introduced into intron 2 of the *V2R* gene. A third loxP site was inserted into intron 1. Heterozygous V2R mutant mice (females) in which 1 WT V2R allele was replaced with the $loxP^{neo}$-modified version of the gene ($V2R^{+/fl^{neo}}$) were obtained by standard mouse gene–targeting techniques (Figure 1, A and B). In the next step, the *neo* cassette was removed by crossing $V2R^{+/fl^{neo}}$ mice with *EIIa-Cre* transgenic mice, which express Cre recombinase in the early embryo (14). Female mice heterozygous for the floxed V2R allele ($V2R^{fl/+}$) lacking both the *neo* cassette and the *EIIa-Cre* transgene were then crossed to *Esr1-Cre* transgenic mice, which express a tamoxifen-inducible Cre recombinase/mutant estrogen receptor fusion protein under the transcriptional control of a strong general promoter (chicken β-actin promoter; refs. 15, 16). This mating schedule yielded mice of different genotypes including male hemizygous V2R mutant pups harboring the *Esr1-Cre* transgene ($V2R^{fl/y}$*Esr1-Cre* mice). Male $V2R^{fl/y}$ mice lacking the *Esr1-Cre* transgene were used as control animals in most experiments. All genotypes were obtained at the expected Mendelian frequency.

To disrupt the *V2R* gene in $V2R^{fl/y}$*Esr1-Cre* mice, 7- to 8-week-old male mice received daily injections of 4-OH-tamoxifen (TMX) (0.5 mg i.p./mouse) for 6 consecutive days. PCR analysis of genomic DNA prepared from kidneys of TMX-injected mice of different genotypes confirmed that TMX treatment led to the deletion of coding exon 2 only in $V2R^{fl/y}$*Esr1-Cre* mice (Figure 1C). To confirm the absence of functional V2Rs in kidneys of TMX-treated $V2R^{fl/y}$*Esr1-Cre* mice, we carried out [^{3}H]-AVP saturation binding studies using whole-kidney membrane homogenates. Since the

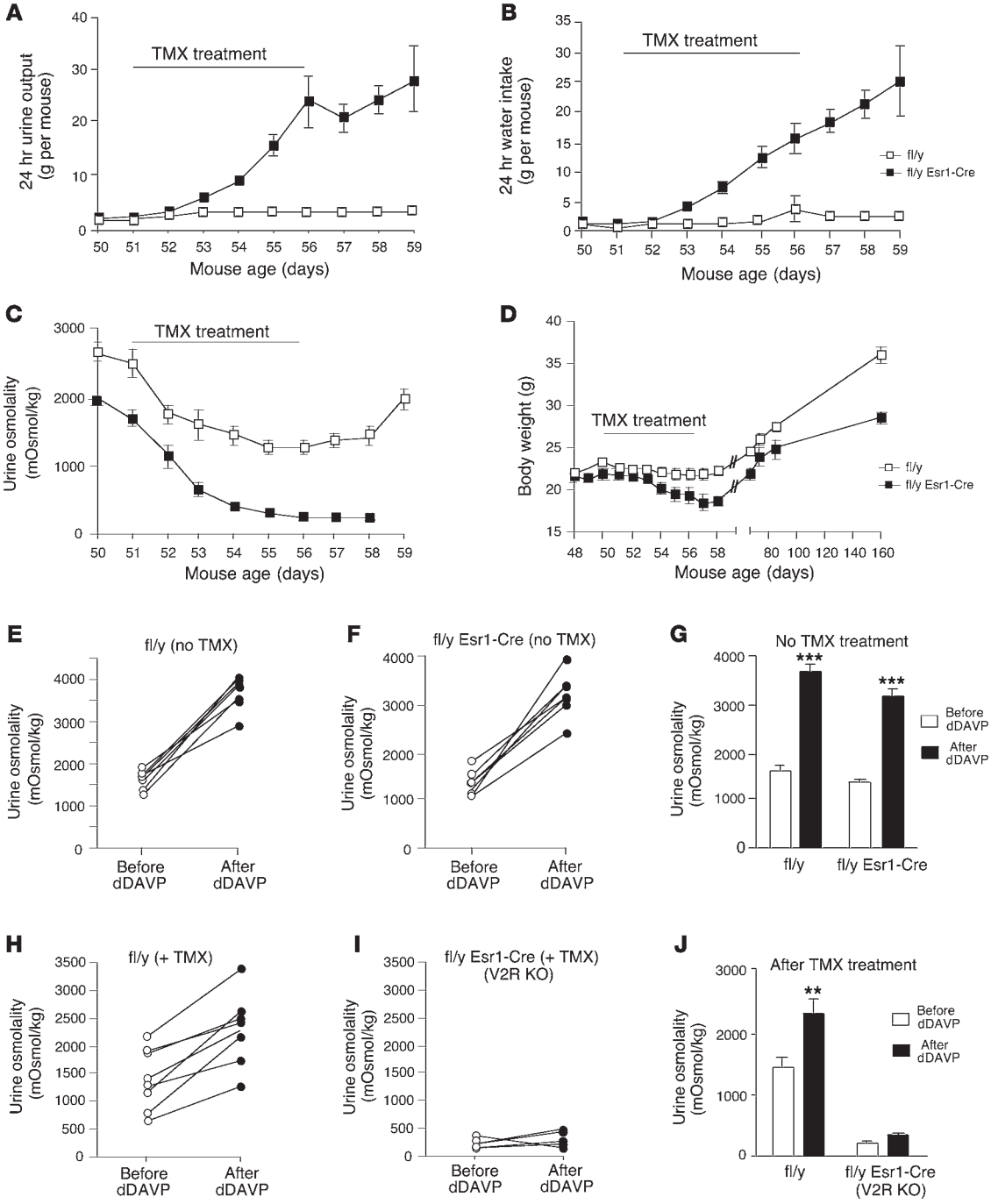

Figure 2

Loss of urinary concentrating ability in V2R-KO mice. (**A** and **B**) 24-hour urine output and water consumption of V2R mutant mice and control littermates. *V2R$^{fl/y}$Esr1-Cre* mice and *V2R$^{fl/y}$* control littermates were injected at the indicated days with a single dose of TMX (0.5 mg i.p./mouse). Daily urine output (**A**) and water consumption (**B**) were determined at the indicated days by using metabolic cages. (**C** and **D**) Urine osmolality and body weight of *V2R$^{fl/y}$Esr1-Cre* mice and control littermates. (**E**–**J**) Urine-concentrating ability of dDAVP. Urine osmolalities were determined immediately before and 1.5–2 hours after a single injection of dDAVP (0.4 μg/kg, i.p.). (**E** and **F**) Data obtained with individual *V2R$^{fl/y}$* and *V2R$^{fl/y}$Esr1-Cre* mice that had not been treated with TMX are shown (mouse age, 7 weeks). (**G**) Summary of the data shown in **E** and **F**. (**H** and **I**) Data obtained with individual TMX-treated *V2R$^{fl/y}$* mice (controls) and *V2R$^{fl/y}$Esr1-Cre* mice (V2R-KO mice; mouse age, 9 weeks). (**J**) Summary of data depicted in **H** and **I**. Data are shown as mean ± SEM. n = 5–7 per group.**P < 0.01; ***P < 0.001.

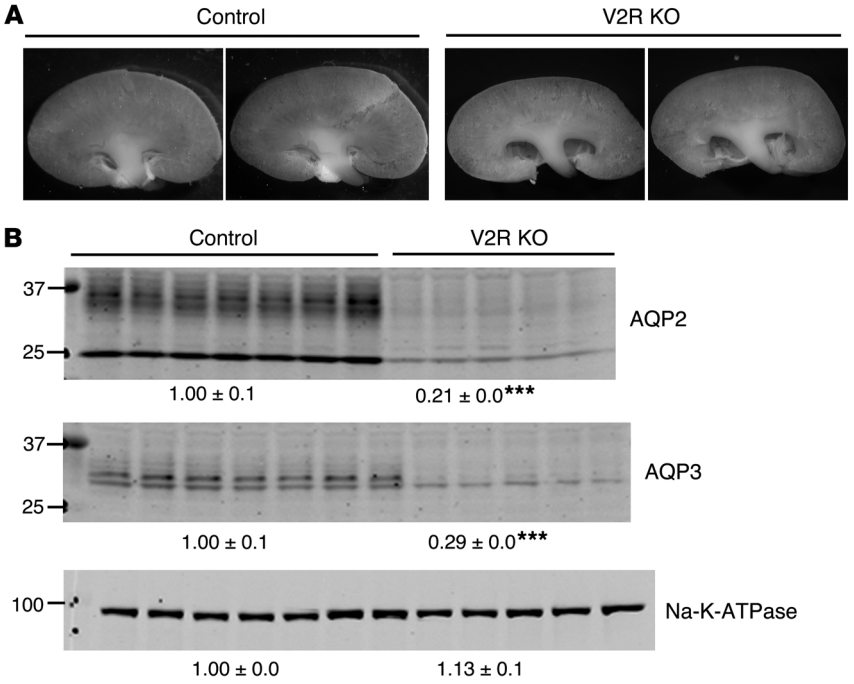

Figure 3
Distension of the renal pelvis and reduced renal AQP2 and AQP3 expression levels in V2R-KO mice. (**A**) Kidney morphology. Right kidneys were resected and photographed. Representative photographs of kidneys from control littermates (TMX-treated *V2R$^{fl/y}$* mice) and V2R-KO mice (TMX-treated *V2R$^{fl/y}$Esr1-Cre* mice) are shown (mouse age, 8 months). (**B**) Immunoblots assessing protein abundance of the collecting duct aquaporin water channels AQP2 and AQP3. V2R-KO mice and control littermates (TMX-treated *V2R$^{fl/y}$* mice) were sacrificed 6 months after TMX treatment. Homogenates prepared from whole left kidneys were used for Western blotting studies. Na-K-ATPase was also detected via immunoblotting for control purposes. Values are mean band densities ± SEM normalized by defining the means of the control samples as 1 (V2R-KO, n = 5; control, n = 7). Note that renal AQP2 and AQP3 expression levels were significantly reduced in V2R-KO mice. ***P < 0.001.

kidney also expresses low levels of V1a vasopressin receptors (17) and [^{3}H]-AVP binds to all vasopressin receptor subtypes, all binding studies were carried out in the presence of the selective V1a receptor antagonist, HO-LVA (2 nM; refs. 18, 19). This analysis showed that kidney preparations from TMX-treated control mice (*V2R$^{fl/y}$* mice) bound [^{3}H]-AVP with high affinity (K_d = 0.73 ± 0.06 nM) and a B_{max} value (maximum receptor density) of 54 ± 11 fmol/mg membrane protein (n = 3; Figure 1D). In striking contrast, kidney membranes prepared from TMX-treated *V2R$^{fl/y}$Esr1-Cre* mice were completely devoid of specific [^{3}H]-AVP–binding activity (n = 4; Figure 1D), confirming that TMX-induced activation of the Esr1-Cre fusion protein led to the effective disruption of the *V2R* gene in V2R-expressing kidney cells. Thus, for the sake of simplicity, TMX-treated *V2R$^{fl/y}$Esr1-Cre* mice are referred to as V2R-KO mice in the following.

Conditional V2R-KO mice exhibit sustained excretion of large amounts of hypotonic urine. Male *V2R$^{fl/y}$Esr1-Cre* mice and control littermates (*V2R$^{fl/y}$* mice) (mouse age, 7 to 8 weeks) were placed into metabolic cages, and 24-hour urine production and water intake were monitored over 10 days. Each mouse received a single daily injection of TMX (0.5 mg i.p./mouse) for a 6-day period. Prior to TMX administration, urine output and water consumption were not statistically different between the 2 groups of mice (however, *V2R$^{fl/y}$Esr1-Cre* showed a slight trend to an increased urine output and water intake; P > 0.05; Figure 2, A and B). The TMX injections had no significant effect on these 2 variables in control mice (Figure 2, A and B). In contrast, TMX treatment of *V2R$^{fl/y}$Esr1-Cre* mice led to a time-dependent, dramatic increase in urine production and water intake (Figure 2, A and B). At the end of the 10-day observation period, TMX-treated *V2R$^{fl/y}$Esr1-Cre* mice displayed pronounced polyuria and polydipsia, producing approximately 25–30 g of urine and consuming about the same amount of water per day (Figure 2, A and B). Figure 2C shows that the urine produced by TMX-treated *V2R$^{fl/y}$Esr1-Cre* mice had a very low osmolality (175 ± 18 mOsmol/kg; n = 5). These data are in agreement with the observation that TMX treatment of *V2R$^{fl/y}$Esr1-Cre* mice leads to a complete loss of renal V2R-binding activity (Figure 1D).

We also noted that the urine osmolality of the *V2R$^{fl/y}$Esr1-Cre* mice was significantly lower (by ~25%) than that of the control mice even prior to TMX treatment (day 50, P < 0.01; Figure 2C). One possible explanation for this phenomenon is that the *Esrl-Cre* transgene is slightly "leaky," displaying a small degree of TMX-independent Cre activity (15).

Consistent with the urine osmolality measurements, TMX-mediated deletion of the *V2R* gene resulted in dramatic reductions in urine urea, creatinine, and Na^+ and K^+ concentrations (Supplemental Table 1; supplemental material available online with this article; doi:10.1172/JCI39680DS1). However, the serum Na^+ levels of V2R-KO mice remained in a physiological range (serum Na^+ is the major determinant of serum osmolality). The serum Na^+ levels of *V2R$^{fl/y}$Esr1-Cre* mice measured 2 weeks before and 2 weeks after the TMX injection period amounted to 146 ± 1 and 149 ± 1 mEq/l, respectively (mean ± SEM; n = 7).

V2R-KO mice also showed reduced weight gain, as compared with their TMX-treated control littermates. Figure 2D shows that 160-day-old V2R-KO mice weighed approximately 25% less than the control animals, probably due to the physiological stress caused by the XNDI phenotype. Most importantly, TMX-induced deletion of the *V2R* gene resulted in viable V2R-KO mice, in contrast with mutant V2R mice lacking functional V2Rs throughout development (12).

We next measured urine osmolalities in response to a single injection (0.4 μg/kg, i.p.) of 1-desamino-8-D-AVP (dDAVP), a selective V2R agonist. Prior to TMX treatment, *V2R$^{fl/y}$Esr1-Cre* mice and control littermates (*V2R$^{fl/y}$* mice) were able to concentrate their urine to a similar extent in response to dDAVP (Figure 2, E–G). Similarly, dDAVP administration led to a significant increase in urine osmolality in TMX-treated control mice (Figure 2, H and J). In striking contrast, dDAVP treat-

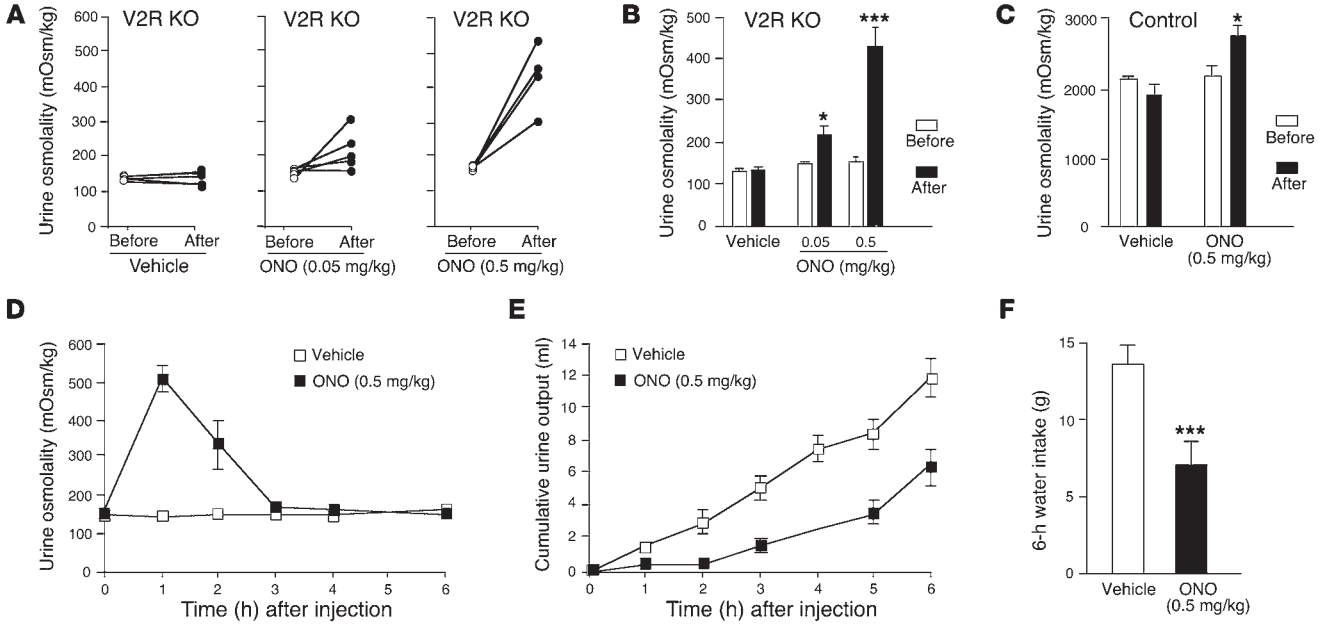

Figure 4

Acute effects of ONO on urine osmolality, urine output, and water consumption. (**A** and **B**) Acute urine-concentrating effect of ONO. V2R-KO mice (TMX-treated *V2R$^{fl/y}$Esr1-Cre* mice; age, 6.5 months) received a single dose of ONO (0.05 or 0.5 mg/kg s.c.) or vehicle (n = 4 or 5). Urine was collected immediately before and 1.5–2 hours after ONO or vehicle injection. (**A**) Urine osmolality data obtained with individual mice are shown. (**B**) Summary of data shown in **A**. (**C**) Summary of urine osmolality data obtained with ONO-treated control mice. Control mice (TMX-treated *V2R$^{fl/y}$* mice; age, 6.5 months) received a single dose of ONO (0.5 mg/kg s.c.; n = 6) or vehicle (n = 9). (**D**) Time course of changes in urine osmolality measured in ONO-treated V2R-KO mice. V2R-KO mice (age, 7 months) were treated with either vehicle (n = 5) or ONO (0.5 mg/kg s.c., n = 6). (**E**) Cumulative urine production measured in ONO-treated V2R-KO mice. V2R-KO mice (age, 7 months) were injected with ONO (0.5 mg/kg s.c., n = 6) or vehicle (n = 5). (**F**) Water intake of ONO-treated V2R-KO mice. V2R-KO mice (age, 7 months) were injected with ONO (0.5 mg/kg s.c., n = 6) or vehicle (n = 5). Water intake was measured 6 hours after injection. Data are shown as mean ± SEM. *P < 0.05; ***P < 0.001.

ment was unable to increase urine osmolality in TMX-treated *V2R$^{fl/y}$Esr1-Cre* mice (Figure 2, I and J), consistent with the lack of renal V2Rs (Figure 1D).

Conditional V2R-KO mice show changes in renal morphology and reduced renal AQP2 and AQP3 expression levels. To determine whether the inducible deletion of the *V2R* gene led to changes in kidney morphology, right kidneys from TMX-treated *V2R$^{fl/y}$Esr1-Cre* mice (n = 5) and control littermates (*V2R$^{fl/y}$* mice; n = 7) were resected and photographed (mouse age, 8 months). We found that all kidneys prepared from V2R-KO mice, but none of the kidneys obtained from the control mice, displayed a considerable distension of the renal pelvis (representative photographs are shown in Figure 3A).

V2R activity is known to regulate the expression levels of various renal proteins critical for urine concentration, including different sodium channels and the AQP2 and AQP3 water channels (for a recent review, see ref. 20). Immunoblotting studies showed that AQP2 and AQP3 expression levels were drastically reduced (by ~70%–80%) in V2R-KO mice as compared with control mice (mouse age, 8 months; Figure 3B). In contrast, conditional deletion of the *V2R* gene had no significant effect on the protein expression levels of the Na-K-2Cl cotransporter (NKCC2), the Na-Cl cotransporter (NCC), and the epithelial sodium channel subunits β-ENaC and γ-ENaC (Supplemental Figure 1).

Mouse inner medullary collecting duct cells express the G_s-coupled EP4 PGE_2 receptor. The V2R is a G_s-coupled receptor, and G_s-mediated cAMP production is known to be essential for the antidiuretic activity mediated by this receptor subtype. We speculated that renal collecting duct cells might express other G_s-coupled receptors that could serve as potential targets ("V2R bypasses") for the treatment for XNDI. To determine which GPCRs are expressed by mouse inner medullary collecting duct (IMCD) cells, we first prepared total RNA from IMCD tubule suspensions using C57BL/6 WT mice (10-week-old males). We then measured receptor expression levels via real-time quantitative RT-PCR (qRT-PCR) using mouse GPCR array plates containing specific primers and TaqMan probes for all mouse GPCRs, except for the odorant, taste, and pheromone receptors. These studies showed that mouse IMCD cells express many GPCRs including the V2R, which proved to be the most highly expressed GPCR (Supplemental Table 2). Besides the V2R, this analysis identified 1 additional G_s-coupled receptor that was expressed in mouse IMCD cells at significant levels, the EP4 subtype of the PGE_2 receptor (or short EP4 receptor; Supplemental Table 2). Real-time qRT-PCR analysis showed that the TMX-induced deletion of the *V2R* gene had no significant effects on EP4 receptor transcript levels in mouse IMCD cells (data not shown).

A single injection of ONO, a selective EP4 receptor agonist, ameliorates the key manifestations of XNDI. To test the possibility that stimulation of renal EP4 receptors is beneficial for the treatment of XNDI, V2R-KO mice (TMX-treated *V2R$^{fl/y}$Esr1-Cre* mice; age, 7 months) were given a single dose of the selective EP4 receptor agonist ONO (0.05 or 0.5 mg/kg s.c.; ref. 13). Figure 4, A and B, shows that ONO treatment led to dose-dependent increases in urine osmolality in V2R-KO mice (urine osmolalities were measured immediately before and 1.5–2

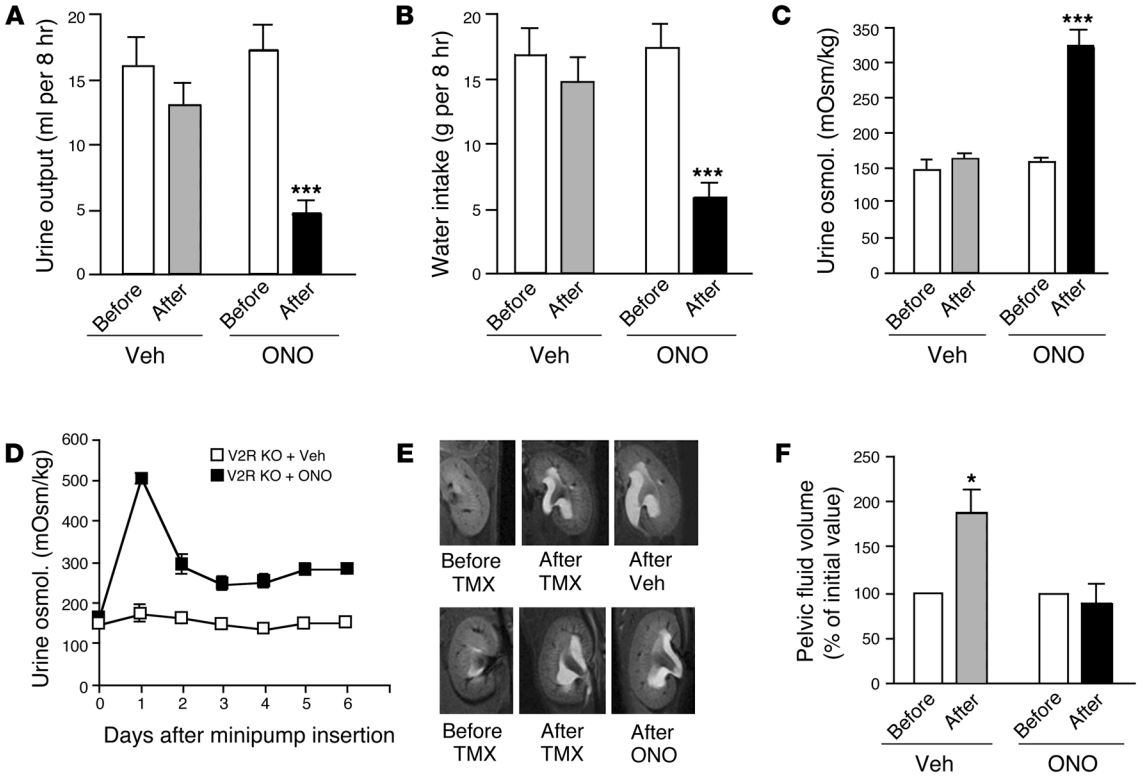

Figure 5

Effects of prolonged treatment of V2R-KO mice with ONO on urine output, water intake, urine osmolality, and kidney morphology. (**A** and **B**) Urine output and water intake measurements. One day after the end of the TMX-injection period, V2R-KO mice received either vehicle or ONO (55 μg daily per mouse) via s.c. infusion for 9 days, followed by urine output (**A**) and water consumption (**B**) measurements (n = 4 or 5). (**C**) Urine osmolality measurements. Urine samples collected during the experiments shown in **A** and **B** were used for these measurements (n = 4 or 5). (**D**) Urine osmolality of vehicle- or ONO-treated V2R-KO mice over a 6-day period. Five days after the end of the TMX-injection period, V2R-KO mice received either vehicle or ONO (55 μg daily per mouse) via s.c. infusion (n = 4-6). (**E**) MRI images of kidneys from *V2R$^{fl/y}$Esr1-Cre* mice. Five days after the end of the TMX-injection period, V2R-KO mice received either vehicle or ONO (55 μg daily per mouse) via s.c. infusion for 2 weeks. Cavities where the contrast agent (Magnevist) accumulates in fluid appear white on the MRI (see Methods for experimental details). Representative images are shown (n = 4 per group). (**F**) Quantification of MRI images shown in **E**. Data are presented as mean ± SEM. *P < 0.05; ***P < 0.001. Veh, vehicle.

hours after ONO injection). The higher ONO dose (0.5 mg/kg) increased urine osmolalities in V2R-KO mice by approximately 2.5-fold (Figure 4B). Treatment of control littermates (TMX-treated *V2R$^{fl/y}$* mice) with 0.5 mg/kg of ONO led to a much smaller (~1.2-fold) increase in urine osmolalities (Figure 4C).

To obtain information about the duration of the urinary concentrating effects of ONO, we injected V2R-KO mice with 0.5 mg/kg (s.c.) of ONO and monitored urine osmolalities and cumulative urine output over a 6-hour period. V2R-KO mice showed an approximately 3-fold increase in urine osmolality 1 hour after ONO injection and an approximately 2-fold increase in urine osmolality at the 2-hour time point (Figure 4D). At later time points, urine osmolalities returned to baseline values (~160 mOsmol/kg; Figure 4D), indicating that ONO has a relatively short biological half-life in mice (<3 hours). However, at present, no pharmacokinetic data are available for ONO (Takayuki Maruyama, personal communication).

Consistent with the urine osmolality measurements, urine output was dramatically reduced in V2R-KO mice during the first 2 hours after ONO injection (Figure 4E). At the end of the 6-hour observation period, cumulative urine output was approximately 50% lower in ONO-treated than in vehicle-treated V2R-KO mice (Figure 4E). At the same time point, cumulative water consumption was also decreased by approximately 50% in ONO-treated V2R-KO mice, as compared with vehicle-treated V2R-KO mice (Figure 4F). Taken together, these findings indicate that ONO is highly efficacious in increasing urine osmolality and reducing urine output and water consumption in the absence of V2Rs.

Beneficial effects of prolonged ONO treatment in XNDI mutant mice. Since a single s.c. injection of ONO had only a relatively short-lasting effect (Figure 4D), we infused V2R-KO mice (TMX-treated *V2R$^{fl/y}$Esr1-Cre* mice; age, 3 months) with ONO by using osmotic minipumps for up to 3 weeks (55 μg ONO/d/mouse s.c.). Prolonged ONO infusion led to a striking reduction in urine output and water intake of V2R-KO mice and a concomitant increase in urine osmolality, as compared with preinfusion values (Figure 5, A–D). The increase in urine osmolality was most pronounced after the first day of ONO infusion (Figure 5D). Since chronic stimulation of GPCRs is known to trigger multiple cellular events that dampen tissue responses in the continued presence of an activating ligand (receptor desensitization), one possibility is that receptor desensitization events are responsible for the observation that the ONO effects on urine osmolality were reduced at later time points (Figure 5D).

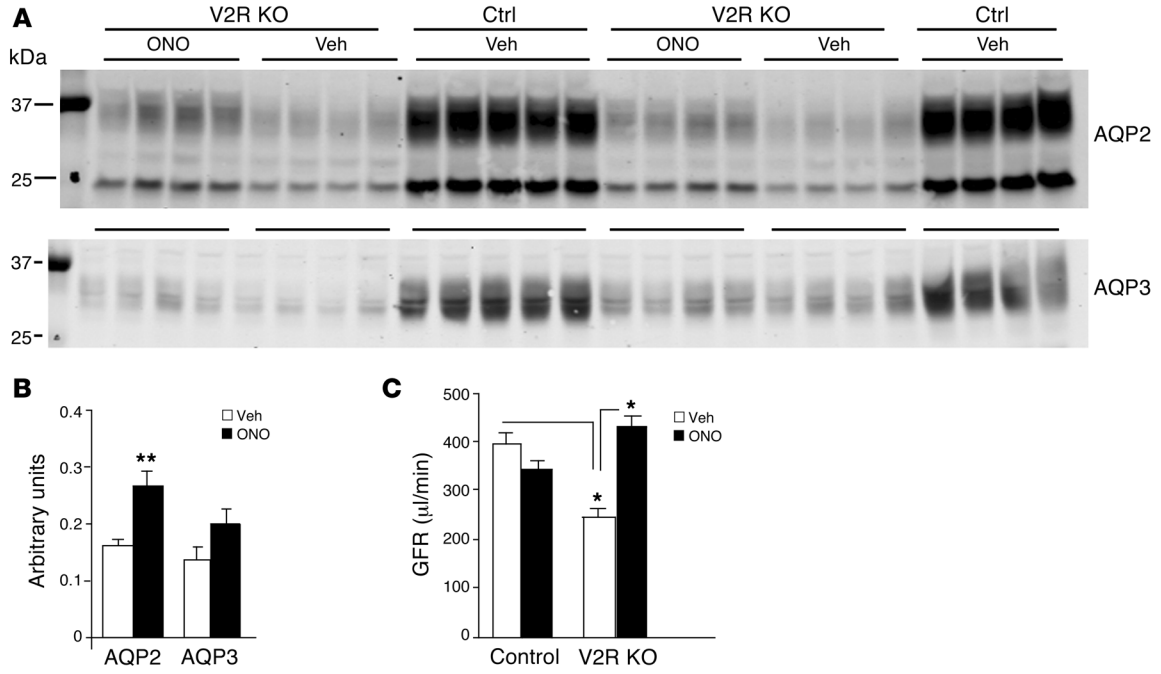

Figure 6
Effects of prolonged treatment of V2R-KO mice with ONO on renal AQP2 and AQP3 expression levels and GFR. (**A** and **B**) Immunoblotting studies examining the effect of chronic ONO treatment of V2R-KO mice on AQP2 and AQP3 expression levels. Five days after the end of the TMX-injection period, V2R-KO mice received either vehicle or ONO (55 μg/d/mouse) via s.c. infusion for 2 weeks. Subsequently, Western blotting studies were carried out using homogenates prepared from whole left kidneys (**A**). TMX-treated *V2R*$^{fl/y}$ mice were used as controls. Samples were loaded in duplicate. (**B**) Summary of immunoblotting data shown in **A**. Values represent mean band densities ± SEM in V2R-KO mice normalized by defining the means of the vehicle-treated control samples as 1. (**C**) GFR measurements. V2R-KO mice and control littermates (TMX-treated *V2R*$^{fl/y}$ mice) received either vehicle or ONO (55 μg/d/mouse) via s.c. infusion for up to 10 days (n = 4–6 per group). GFR measurements were carried out in conscious mice as described under Methods. Data are presented as mean ± SEM. *P < 0.05; **P < 0.01.

To determine whether prolonged ONO treatment had any effect on the pathological changes in kidney morphology usually associated with XNDI, we employed MRI that relies on the ability of a chelated gadolinium contrast agent to accumulate in the urinary space (21). *V2R*$^{fl/y}$*Esr1-Cre* mice received either vehicle or ONO (55 μg/d/mouse) via s.c. infusion for 2 weeks using osmotic minipumps. Mice were serially imaged, first before the 6-day TMX injection period, then 3 days after the last TMX injection, and finally 2 weeks after the start of vehicle or ONO infusion (infusions were initiated 5 days after the last TMX injection). In vehicle-treated V2R-KO mice, the distension of the renal pelvis caused by TMX-mediated disruption of the *V2R* gene became more pronounced during the course of the experiment (Figure 5, E and F). Figure 5F shows that the volume of pelvic fluid increased by approximately 2-fold during the 2-week vehicle infusion period. In contrast, ONO treatment of V2R-KO mice completely prevented the further expansion of renal pelvic space (Figure 5, E and F).

Immunoblotting studies showed that s.c. ONO treatment (55 μg/d/mouse) of V2R-KO mice for 2 weeks increased renal AQP2 levels by approximately 70% (P < 0.01; Figure 6, A and B). Mean AQP3 levels were also increased by approximately 40% after the 2-week ONO infusion period (this effect, however, failed to reach statistical significance; P = 0.12; Figure 6, A and B).

Analysis of the mechanism underlying the beneficial effects of ONO in the treatment of XNDI mice. As already mentioned above, the antidiuretic activity of the V2R depends on its ability to activate the stimulatory G protein, G_s, leading to increased cAMP levels, which, via a cascade of biochemical events, eventually trigger an increase in water permeability of the kidney collecting duct cells. Like the V2R, the EP4 prostanoid receptor is a G_s-coupled receptor (22, 23) that is expressed in mouse collecting duct cells (Supplemental Table 2). Consistent with this observation, treatment of WT mouse IMCD tubule suspensions with either ONO or dDAVP led to concentration-dependent increases in intracellular cAMP levels (Figure 7, A and B). The magnitude of the dDAVP-mediated cAMP response was greater than that of the corresponding ONO response, probably as a consequence of the very high V2R expression levels in IMCD cells (Supplemental Table 2).

To study the effect of ONO on the water permeability of kidney collecting duct cells, cortical collecting duct segments were microdissected from rat kidneys and perfused in vitro using an isolated tubule microperfusion technique (24). Osmotic water permeability (P_f in μm/s) was measured fluorometrically using a fluorescent luminal marker (fluorescein sulfonate). Consistent with the in vitro cAMP measurements (Figure 7A), incubation of isolated tubules with ONO (100 nM) led to an approximately 2.5-fold increase in water permeability (P_f in μm/s: control, 35 ± 33; ONO, 83 ± 31; n = 5 per group [preparations were obtained from 5 different animals]; P < 0.05).

In vivo studies showed that chronic s.c. infusion of V2R-KO mice with ONO (55 μg daily per mouse) had no significant effect on diastolic and systolic blood pressure and heart rate (Supplemental Figure 2), excluding the possibility that altered cardiovascular

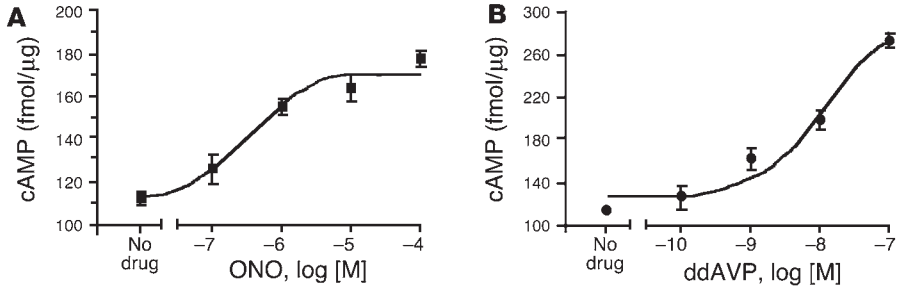

Figure 7

ONO- and dDAVP-induced cAMP production in mouse IMCD tubule suspensions. (**A** and **B**) Drug-induced increases in cAMP levels in mouse IMCD tubule suspensions. Freshly isolated IMCD tubule suspensions from C57BL/6 WT mice (10-week-old males; $n = 7$ per individual experiment) were pooled and equally distributed into 24-well plates. Samples were treated with the indicated concentrations of ONO (**A**) or dDAVP (**B**) for 30 minutes at 37°C. Total cAMP generated in each well was normalized to the amount of protein present in each well. Four independent experiments were carried out. Data are provided as mean ± SEM.

parameters are responsible for the ability of ONO to reduce urine output in the absence of functional V2Rs. Moreover, prolonged ONO treatment of V2R-KO mice had no significant effect on food intake, strongly suggesting that ONO does not cause general malaise (Supplemental Figure 3).

Finally, to exclude the possibility that the ONO-induced decrease in urinary output in V2R-KO mice was due to a reduction in glomerular filtration rate (GFR), we carried out GFR measurements using conscious V2R-KO mice and control littermates (TMX-treated *V2R*$^{fl/y}$ mice) chronically treated (s.c.) with either vehicle or ONO (55 μg/d/mouse) via osmotic minipumps. Vehicle-treated control mice showed a GFR of 395 ± 26 μl/min (Figure 6C). The GFR of ONO-treated control mice was not significantly different from this value (344 ± 14 μl/min; Figure 6C). In contrast, vehicle-treated V2R-KO mice showed a significant reduction (by ~40%) of GFR (246 ± 18 μl/min), as compared with vehicle-treated control mice ($P < 0.05$; Figure 6C). Remarkably, infusion of V2R-KO mice with ONO restored normal GFR (428 ± 26 μl/min; Figure 6C).

Taken together, these observations demonstrate that the beneficial effects of ONO in ameliorating the symptoms of XNDI in V2R-KO mice are due to activation of EP4 prostanoid receptors expressed by renal collecting duct cells.

Discussion

In this study, we describe what we believe is the first viable mouse model of XNDI, the most common form of congenital NDI. In these newly developed mutant mice, the *V2R* gene can be deleted in a conditional (TMX-dependent) fashion in the kidneys of adult mice. The resulting V2R-KO mice showed all key symptoms of XNDI, including the production of large amounts of dilute urine (polyuria) and polydipsia. Following dDAVP administration, the V2R mutant mice were unable to increase their urine osmolality, consistent with the complete absence of renal V2R-binding sites observed in radioligand-binding assays.

Kidneys from V2R-KO mice also showed a distension of the renal pelvis, a characteristic morphological deficit that is generally observed with NDI mutant mice (12, 16, 25–29). Moreover, immunoblotting studies showed that renal AQP2 and AQP3 expression levels were drastically reduced (by ~70%–80%) in V2R-KO mice. The kidney collecting duct AQP2 and AQP3 water channels are known to play a key role in mediating AVP-dependent water reabsorption (4, 30–32). These observations strongly suggest that human XNDI is also associated with pronounced decreases in AQP2 and AQP3 expression levels.

In addition, conscious V2R-KO mice showed an approximately 40% reduction in GFR (as compared with control littermates), despite having normal blood pressure. This observation is clearly of potential clinical interest, since no systematic GFR measurements have been carried out in XNDI patients (Daniel Bichet, unpublished observations). The precise mechanism underlying this phenotypic change remains unclear at present, but this effect may be secondary to chronic polyuria and dilatation of the renal pelvis with urinary reflux.

Current drug treatment strategies for XNDI are problematic and nonspecific in nature. They include the administration of thiazide diuretics (e.g., hydrochlorothiazide [HCT]) along with a reduction in salt intake, frequently in combination with prostaglandin synthesis inhibitors (e.g., indomethacin) or potassium-sparing diuretics (e.g., amiloride) (1–3). However, these drugs only lead to a moderate reduction in urine production, and their use is often associated with severe side effects, including disturbances in electrolyte balance as well as renal and gastrointestinal complications (1, 2). Moreover, in XNDI, thiazides and indomethacin are predicted to reduce GFR (3), thereby increasing the risk of nephropathy. Thus, there is a clear need for new classes of XNDI drugs endowed with increased efficacy and reduced side effects.

We speculated that renal collecting duct cells might express G_s-coupled receptors (besides the V2R) that could serve as more specific targets for the pharmacotherapy of XNDI. Real-time qRT-PCR studies using mouse GPCR array plates demonstrated that mouse IMCD cells express another G_s-coupled receptor (besides the V2R), the EP4 prostanoid receptor, at significant levels. This receptor subtype has also been shown to be expressed by rat IMCD cells (33). The EP4 receptor is one of the 4 receptor subtypes through which PGE_2 exerts its pharmacological actions (22, 23).

To test the potential usefulness of EP4 receptor agonists for the therapy of XNDI, we treated V2R-KO mice with ONO, a drug that is commonly used to study EP4 receptor function. Importantly, ONO is endowed with a very high degree of selectivity for the EP4 receptor subtype (13, 34). Remarkably, both acute and chronic treatment of V2R mutant mice with ONO greatly reduced all major manifestations of XNDI, leading to striking reductions in urine output and water intake and pronounced increases in urine osmolality.

Long-term complications of XNDI include large dilatations of the renal pelvic space as well as kidney failure secondary to bilateral hydronephrosis (1, 2, 5). Interestingly, MRI studies showed that prolonged ONO treatment of V2R-KO mice could prevent the further progression of renal pelvic distension associated with the polyuric state caused by the disruption of the *V2R* gene.

As mentioned above, V2R-KO mice displayed an approximately 40% reduction in GFR. Interestingly, prolonged treatment of V2R-KO mice with ONO restored normal GFR, excluding the possibility that the ONO-mediated decrease in urine output in V2R-KO mice

is simply the consequence of reduced GFR. The ONO-mediated normalization of GFR in V2R-KO mice may provide an additional benefit for the potential treatment of XNDI, since it reduces the risk of nephropathy associated with the use of current XNDI drugs (see above). The ONO-mediated increase in GFR observed in the absence of functional V2Rs may be due to EP4 receptor–mediated vasodilator effects on afferent renal arterioles (35, 36).

Chronic ONO treatment had no effect on blood pressure, heart rate, and food intake, excluding the possibility that changes in cardiovascular parameters or general malaise contributed to the ONO-mediated decrease in urine output.

Immunoblotting studies demonstrated that prolonged treatment of V2R-KO mice with ONO increased renal AQP2 levels by approximately 70%, probably due to EP4 receptor–mediated elevations of cAMP levels in kidney collecting duct cells (20, 37–39). Since AQP2 plays a key role in renal water reabsorption (4, 30–32), this observation is of considerable therapeutic relevance.

ONO treatment of collecting duct tubule preparations led to a pronounced increase in cAMP levels and enhanced water permeability. Taken together, these data support the concept that the beneficial effects of ONO in the treatment of XNDI mice are due to a direct action on EP4 receptors expressed by kidney collecting duct cells.

ONO is relatively unstable in aqueous solution (Takayuki Maruyama, unpublished observations). Moreover, due to the limited solubility of ONO, we could not deliver more than 55 μg of ONO per day (per mouse) in the chronic infusion experiments. These factors may explain why ONO only partially reversed the phenotypic changes displayed by the XNDI mutant mice. The development of more stable EP4 receptor agonists with improved pharmacokinetic properties is therefore likely to yield agents that exhibit increased efficacy in the treatment of XNDI. However, it should be noted that even a drug that shows only moderate activity in reducing urine flow is likely to significantly improve the quality of life of individuals suffering from XNDI.

Whereas ONO-mediated activation of renal EP4 receptors leads to reduced urine output, intrarenal PGE_2 infusion is known to promote diuresis (40), probably via activation of other PGE_2 receptor subtypes mediating inhibition of salt and water absorption along the nephron (22). Inhibition of these latter PGE_2 effects by indomethacin, which reduces tissue PGE_2 levels via nonselective inhibition of cyclooxygenase 1 and 2, is thought to contribute to the ability of this drug to reduce urine production in XNDI patients.

It should be noted that the EP4 receptor is not only expressed in the kidney, but also in several other organs and cell types (23). Studies with EP4 receptor–deficient mice and EP4 receptor–selective agonists have shown that EP4 receptors play a role in facilitating the closure of the ductus arteriosus in newborns, promoting bone growth, protecting against inflammatory bowel disease, and facilitating the migration and maturation of Langerhans cells in the skin as well as in several other physiological functions (23).

Interestingly, GPCR expression analysis demonstrated that mouse IMCD cells also express many orphan GPCR transcripts (Supplemental Table 2). The identification of activating ligands for these receptors might reveal novel G_s-coupled receptors as potential targets for the treatment of XNDI. Moreover, in a recent review, Bouley et al. (39) proposed a number of new strategies that might prove useful for the treatment of NDI by bypassing V2R signaling. The potential clinical usefulness of these various strategies can now be tested in the newly generated XNDI mutant mice.

Whereas most patients with congenital NDI harbor inactivating mutations in the *V2R* gene, a small subpopulation of these patients (~10%) exhibit mutations in the *AQP2* gene, causing NDI with either autosomal dominant or recessive inheritance (2, 4, 31). As has been observed with V2R-KO mice, inactivation of the *AQP2* gene in mice throughout development results in neonatal death (25, 27). However, several viable mouse models of the autosomal form of congenital NDI have been generated recently (16, 26–29, 32, 41).

In conclusion, we have generated what we believe is the first viable mouse model of human XNDI. Our data support the concept that selective EP4 receptor agonists may represent a new class of drugs useful for the treatment of XNDI due to their direct action on kidney collecting duct cells. The newly generated V2R mutant mice should prove generally useful for testing new strategies for the treatment of XNDI.

Methods

Mouse maintenance and diet. Mice were housed in a specific pathogen–free barrier facility (4 to 5 mice per cage) and maintained on a 12-hour light/12-hour dark cycle. Mice were fed ad libitum with a standard mouse chow (4% [w/w] fat content; Zeigler). Bedding and water bottles were replaced daily in cages housing V2R-KO mice. All studies were carried out with male littermates maintained on a C57BL/6 background. All experiments were approved by the Animal Care and Use Committee of the National Institute of Diabetes and Digestive and Kidney Diseases.

Generation of conditional V2R-KO mice. The V2R-targeting construct (Figure 1A) was derived from the pPN2T vector (42) containing a PGK-neomycin resistance gene (*neo* cassette) and 2 copies of the herpes simplex virus thymidine kinase (*HSV-TK*) gene. The mouse V2R coding sequence, which codes for 371 amino acids, is interrupted by 2 short introns, referred to as intron 1 and 2 (Figure 1A). The *neo* cassette, flanked by 2 loxP sequences, was inserted into intron 2, as described by Yun et al. (12) (Figure 1A). In addition, a third loxP site was inserted into intron 1 (185 bp downstream of the ATG start codon). The final targeting construct contained approximately 6 kb of genomic sequence upstream of the first loxP site (5′ arm) and 1.4 kb of genomic sequence downstream of the *neo* gene (3′ arm), respectively.

The newly generated targeting construct (Figure 1A) was linearized with NotI and electroporated into 129 SvEv ES cells (43). G418- and FIAU-resistant clones were isolated and screened for proper integration of the V2R targeting construct via Southern blotting, using BamHI-digested DNA and an external 3′ probe (Figure 1, A and B). Properly targeted ES cell clones were microinjected into C57BL/6 mouse blastocysts to generate chimeric mice. Female chimeric mice were then mated with male WT C57BL/6 mice (Taconic) to obtain F1 offspring. F1 mice containing the floxed V2R allele were identified via Southern blotting (Figure 1, A and B). To eliminate the *neo* cassette, female F1 mice carrying the floxed V2R allele were mated with *EIIa-Cre* transgenic mice (official strain name: B6.FVB-Tg(EIIa-cre)C5379Lmgd/J; genetic background: C57BL/6; The Jackson Laboratory), which express Cre recombinase in the early embryo (14, 44). The successful removal of the *neo* gene was confirmed by PCR analysis of tail genomic DNA using the strategy shown in Figure 1C. Female mice heterozygous for the floxed V2R allele lacking the *neo* cassette were backcrossed to WT male C57BL/6 mice (Taconic) for 2 generations to ensure germline transmission of the mutant *V2R*

gene. In the next step, female mice heterozygous for the floxed V2R allele lacking both the *neo* cassette and the *EIIa-Cre* transgene were crossed to *Esr1-Cre* transgenic mice (official strain name: Tg(cre/Esr1)5Amc/J; genetic background: C57BL/6; The Jackson Laboratory). *Esr1-Cre* transgenic mice express a tamoxifen-inducible Cre recombinase/mouse mutant estrogen receptor fusion protein under the transcriptional control of the chicken β-actin promoter/enhancer coupled with the CMV immediate-early enhancer (15, 16). This mating schedule yielded mice of different genotypes, including male hemizygous V2R mutant pups harboring the *Esr1-Cre* transgene (*V2R$^{fl/y}$Esr1-Cre* mice; conditional V2R-KO mice). Male V2R$^{fl/y}$ mice that did not contain the *Esr1-Cre* transgene served as control animals in most experiments.

Induction of V2R gene deletion. A stock solution of TMX (Sigma-Aldrich) in ethanol (250 mg/ml) was diluted in corn oil to 5 mg/ml. Male *V2R$^{fl/y}$Esr1-Cre* and *V2R$^{fl/y}$* mice (controls) that were 7 to 8 weeks old received single daily i.p. injections of TMX (0.1 ml of a 5 mg/ml suspension) over 6 consecutive days, following a protocol similar to that described by Yang et al. (16).

PCR genotyping analysis. Mouse tail biopsies were used for PCR genotyping studies by using a rapid genotyping kit (Extract-N-Amp Tissue PCR Kit; Sigma-Aldrich). The sequences of the PCR primers used are listed in Supplemental Table 3. The presence of the *Esr1-Cre* transgene was detected by using PCR primers Cre1 and Cre2. The presence of the loxP site in intron 1 was verified by using primers p1 and p2. The successfully removal of the *neo* cassette was confirmed by using primers p3 and p4. The excision of coding exon 2 was verified by using primers p1 and p4. All PCR reactions were run under the following conditions: 94°C for 5 minutes, followed by 31 cycles at 94°C for 45 seconds, 55°C for 30 seconds, and 72°C for 30 seconds. The expected sizes of the different PCR products are indicated in Figure 1C.

Southern blot analysis. A 414-bp PCR product amplified with primers 3.1-F (5′-AATTCATGTTCTGTGCCACAG) and 3.1-R (5′-CACAGGAGCTAAAGCCTGGTA) was used as a probe (3′ probe; Figure 1A). The various recombination events were confirmed by Southern hybridization (Figure 1A). In brief, 10 μg of tail genomic DNA was digested with BamHI, electrophoresed, transferred to a Nylon+ membrane (Schleicher & Schuell BioScience), and hybridized with the ^{32}P-labeled 3′ probe.

Measurement of short-term effects of drugs on urinary osmolality. Urine was collected immediately before and 1.5 to 2 hours after injection of dDAVP (0.4 μg/kg i.p.; Sigma-Aldrich) or ONO (0.05 or 0.5 mg/kg s.c.; gift from Takayuki Maruyama, Ono Pharmaceutical Co. Ltd., Osaka, Japan). Urine samples were collected by placing mice on a wire mesh platform in a clean glass beaker.

Metabolic cage studies and urine osmolality measurements. Urine output and water consumption were measured in metabolic cages (Hatteras Instruments) adapted for mice (for details, see Supplemental Methods). Urine osmolalities were measured via standard procedures using a vapor pressure osmometer (model 5520; Wescor).

Urine and serum chemistry. Blood samples were collected in heparinized glass tubes by puncture of the periorbital venous sinus. Urine and serum chemistry measurements were carried out by the Laboratory of Animal Medicine and Surgery of the National Heart, Lung, and Blood Institute.

[^{3}H]-AVP saturation binding studies. Whole kidneys were collected from 8-month-old male mice, and membrane preparations were obtained essentially as described (12). Membrane preparations (200 μg protein/tube) were incubated with increasing concentrations (0.125–4.0 nM) of [^{3}H]-AVP (61.9 Ci/mmol; PerkinElmer). Incubations were carried out for 2 hours at room temperature. To block renal V1a receptors, 2 nM of HO-LVA (a gift from Maurice Manning, The University of Toledo, Toledo, Ohio, USA), a highly selective V1a receptor antagonist (18, 19), was added to all tubes. Reactions were terminated by rapid filtration over GF/C filters (Brandel). Nonspecific binding was defined as binding in the presence of 5 μM dDAVP. Binding data were analyzed by a nonlinear 1-binding-site curve-fitting procedure using Prism (version 4.0; GraphPad Software Inc.).

Immunoblotting studies. Whole-kidney homogenates were prepared from mouse kidneys and solubilized in Laemmli's reagent. Immunoblotting studies were performed using rabbit affinity-purified polyclonal antibodies, as described previously (45). Thirty μg of protein were loaded per lane. The blots were developed using an Alexa Fluor 680–conjugated secondary antibody (Molecular Probes). Bands were visualized and analyzed using LI-COR's Odyssey infrared imaging system (LI-COR) (45). To facilitate comparisons, we normalized band intensities such that the mean for the control mice was defined as 1 (AU).

Preparation of IMCD tubule suspensions. Mouse IMCD tubule suspensions were prepared as described previously with slight modifications (46). Inner medullas were dissected out from kidneys of C57BL/6 WT mice (10-week-old males), minced, and enzymatically digested in sucrose solution (250 mM sucrose, 10 mM triethanolamine, pH 7.6) containing 3 mg/ml collagenase B and 2000 U hyaluronidase at 37°C for 90 minutes. The resulting suspension was centrifuged at 80 *g* for 30 seconds. IMCD-enriched pellets were harvested after 3 washes with sucrose solution.

cAMP assays. cAMP assays were performed using mouse IMCD tubule suspensions prepared as described above. For each individual experiment, IMCD suspensions were prepared and pooled from the kidneys of 7 C57BL/6 WT mice (10-week-old males). Aliquots of IMCD tubule suspensions were preincubated with the cAMP phosphodiesterase inhibitors 3-isobutyl-1-methylxanthine (IBMX) and Ro-20 (0.1 mM each; Sigma-Aldrich) for 10 minutes at 37°C. Subsequently, different concentrations of ONO (0.1–100 μM) or dDAVP (0.1–100 nM) were added, and reactions were carried out for 30 minutes at 37°C. Total intracellular cAMP was determined via ELISA according to the manufacturer's instructions (cAMP Biotrak; GE Healthcare). Protein concentrations were determined by using the Bradford method (Bio-Rad). cAMP data were analyzed using Prism software (version 4.0; GraphPad Software Inc.).

Microperfusion of isolated renal tubules. Cortical collecting duct segments were freshly microdissected from medullary rays of the kidney of male Sprague-Dawley rats (100–120 g; Taconic Farms), mounted on glass pipettes, and perfused in vitro at 37°C using the technique of Burg (24). Osmotic water permeability (P_f in μm/s) was measured fluorometrically using a fluorescent luminal marker (1 mM of fluorescein sulfonate; Molecular Probes, Invitrogen), as described previously (47). Basal P_f values were obtained after a 30-minute equilibration period. Subsequently, prewarmed bath solution containing the ONO compound was added, and P_f values were determined after an additional 30-minute equilibration period. Three fluid samples were collected for P_f determinations at the end of each of the 2 equilibration periods.

Photography of mouse kidneys. Mouse right kidneys were bisected slightly off the center. Photographic images were taken with a Sony CCD camera (model DKC-5000) mounted on a Wild M-8 dissection microscope.

GFR measurements in conscious mice. GFR was determined in conscious mice by measuring the rate of disappearance of plasma FITC-inulin as previously described (48, 49). In brief, a bolus of approximately 2.5% FITC-inulin (3.7 μl/g body weight; Sigma-Aldrich) was injected retroorbitally under short isoflurane anesthesia, and blood was collected into heparinized 5 μl microcaps (Drummond Scientific) at 3, 7, 10, 15, 35, 55, and 75 minutes after the injection. The collected plasma was diluted 1:10 in 500 mM HEPES (Sigma-Aldrich) of neutral pH, and fluorescence was measured in a Nanodrop-ND-3300 spectrometer (Nanodrop Technologies). GFR was determined by analyzing FITC-inulin plasma disappearance using a 2-compartment model of 2-phase exponential decay.

MRI imaging of mouse kidneys. To detect changes in kidney morphology, MRI experiments were carried out using a 7.0 T, 16-cm horizontal Bruker MR imaging system (Bruker) with Bruker ParaVision 4.0 software. Mice were anesthetized with 1.5%–2.5% isoflurane and imaged using a 38-mm Bruker birdcage volume coil. Respiration and body temperature were monitored via a computerized monitoring system (SA Instruments) throughout the experiment. Gadolinium-DTPA (Gd-DTPA; Magnevist, Berlex) was used as a contrast agent to visualize renal morphology. Magnevist was diluted 1:20 in 0.9% saline and then administered s.c. at a dose of 0.2 mmol/d/kg body weight. T1 weighted spin echo images (TR/TE = 700/10.8 ms, 6 averages, 0.5-mm slice thickness, 11 slices, 2.8 cm × 5.4 cm field of view, 512 × 256 matrix, with fat saturation) were acquired in the coronal plane through the kidneys beginning 10 minutes after Magnevist injection. Mice were imaged serially, first before the 6-day TMX injection period, then 3 days after the last TMX injection, and finally 2 weeks after the start of s.c. delivery of either vehicle or ONO via osmotic minipumps (infusions were initiated 5 days after the last TMX injection). The fluid volume in the kidney showing high signal intensity was calculated using CAAS-MRV_FARM software (Pie Medical Imaging).

Statistics. Data are expressed as mean ± SEM for the indicated number of observations. For comparisons between 2 groups, the paired or unpaired Student's *t* test (2-tailed) was used, as appropriate. For multiple comparisons, 1-way ANOVA was applied. $P < 0.05$ was considered statistically significant.

Acknowledgments

This research was supported by the Intramural Research Program budgets of the National Institute of Diabetes and Digestive and Kidney Disorders (NIDDK) and the National Heart, Lung, and Blood Institute (NHLBI) (project number ZO1-HL-001285). We thank Brenda Klaunberg and Vivian Diaz (In Vivo NMR Center, National Institute of Neurological Disorders and Stroke) for their help with the blood pressure measurements, Shawn Kozlov (NHLBI) for analyzing urine and serum samples, and Cuiling Li and Yinghong Cui (NIDDK) for expert technical assistance.

Received for publication April 27, 2009, and accepted in revised form July 1, 2009.

Address correspondence to: Jürgen Wess, Laboratory of Bioorganic Chemistry, Molecular Signaling Section, National Institute of Diabetes and Digestive and Kidney Diseases, Bldg. 8A, Room B1A-05, 8 Center Drive, Bethesda, Maryland 20892, USA. Phone: (301) 402-3589; Fax: (301) 480-3447; E-mail: jwess@helix.nih.gov.

1. Knoers, N., and Monnens, L.A. 1992. Nephrogenic diabetes insipidus: clinical symptoms, pathogenesis, genetics and treatment. *Pediatr. Nephrol.* **6**:476–482.
2. Bichet, D.G., and Fujiwara, T.M. 1998. Diversity of nephrogenic diabetes insipidus mutations and importance of early recognition and treatment. *Clin. Exp. Nephrol.* **2**:253–263.
3. Oksche, A., and Rosenthal, W. 1998. The molecular basis of nephrogenic diabetes insipidus. *J. Mol. Med.* **76**:326–337.
4. Nielsen, S., Kwon, T.H., Frøkiaer, J., and Agre, P. 2007. Regulation and dysregulation of aquaporins in water balance disorders. *J. Intern. Med.* **261**:53–64.
5. Bichet, D.G. 2008. Vasopressin receptor mutations in nephrogenic diabetes insipidus. *Semin. Nephrol.* **28**:245–251.
6. Holtzman, E.J., and Ausiello, D.A. 1994. Nephrogenic diabetes insipidus: causes revealed. *Hosp. Pract. (Off. Ed.).* **29**:89–93, 97–98, 103–104.
7. Birnbaumer, M. 2001. The V2 vasopressin receptor mutations and fluid homeostasis. *Cardiovasc. Res.* **51**:409–415.
8. Nielsen, S., et al. 1995. Vasopressin increases water permeability of kidney collecting duct by inducing translocation of aquaporin-CD water channels to plasma membrane. *Proc. Natl. Acad. Sci. U. S. A.* **92**:1013–1017.
9. DiGiovanni, S.R., Nielsen, S., Christensen, E.I., and Knepper, M.A. 1994. Regulation of collecting duct water channel expression by vasopressin in Brattleboro rat. *Proc. Natl. Acad. Sci. U. S. A.* **91**:8984–8988.
10. Ecelbarger, C.A., et al. 1995. Aquaporin-3 water channel localization and regulation in rat kidney. *Am. J. Physiol.* **269**:F663–F672.
11. Spanakis, E., Milord, E., and Gragnoli, C. 2008. AVPR2 variants and mutations in nephrogenic diabetes insipidus: review and missense mutation significance. *J. Cell Physiol.* **217**:605–617.
12. Yun, J., et al. 2000. Generation and phenotype of mice harboring a nonsense mutation in the V_2 vasopressin receptor gene. *J. Clin. Invest.* **106**:1361–1371.
13. Suzawa, T., et al. 2000. The role of prostaglandin E receptor subtypes (EP1, EP2, EP3, and EP4) in bone resorption: an analysis using specific agonists for the respective EPs. *Endocrinology.* **141**:1554–1559.
14. Lakso, M., et al. 1996. Efficient in vivo manipulation of mouse genomic sequences at the zygote stage. *Proc. Natl. Acad. Sci. U. S. A.* **93**:5860–5865.
15. Hayashi, S., and McMahon, A.P. 2002. Efficient recombination in diverse tissues by a tamoxifen-inducible form of Cre: a tool for temporally regulated gene activation/inactivation in the mouse. *Dev. Biol.* **244**:305–318.
16. Yang, B., Zhao, D., Qian, L., and Verkman, A.S. 2006. Mouse model of inducible nephrogenic diabetes insipidus produced by floxed aquaporin-2 gene deletion. *Am. J. Physiol. Renal Physiol.* **291**:F465–F472.
17. Ostrowski, N.L., Young, W.S. III, Knepper, M.A., and Lolait, S.T. 1993. Expression of vasopressin V1a and V2 receptor messenger ribonucleic acid in the liver and kidney of embryonic, developing, and adult rats. *Endocrinology.* **133**:1849–1859.
18. Manning, M., et al. 1992. A novel approach to the design of synthetic radioiodinated linear V_{1a} receptor antagonists of vasopressin. *Int. J. Pept. Protein Res.* **40**:261–267.
19. Manning, M., et al. 2008. Peptide and non-peptide agonists and antagonists for the vasopressin and oxytocin V_{1a}, V_{1b}, V_2 and OT receptors: research tools and potential therapeutic agents. *Prog. Brain Res.* **170**:473–512.
20. Fenton, R.A., and Knepper, M.A. 2007. Mouse models and the urinary concentrating mechanism in the new millennium. *Physiol. Rev.* **87**:1083–1112.
21. Jacob, V.A., et al. 2008. Magnetic resonance imaging of urea transporter knockout mice shows renal pelvic abnormalities. *Kidney Int.* **74**:1202–1208.
22. Breyer, M.D., and Breyer, R.M. 2001. G protein-coupled prostanoid receptors and the kidney. *Annu. Rev. Physiol.* **63**:579–605.
23. Sugimoto, Y., and Narumiya, S. 2007. Prostaglandin E receptors. *J. Biol. Chem.* **282**:11613–11617.
24. Burg, M.B. 1972. Perfusion of isolated renal tubules. *Yale J. Biol. Med.* **45**:321–326.
25. Yang, B., Gillespie, A., Carlson, E.J., Epstein, C.J., and Verkman, A.S. 2001. Neonatal mortality in an aquaporin-2 knock-in mouse model of recessive nephrogenic diabetes insipidus. *J. Biol. Chem.* **276**:2775–2779.
26. Lloyd, D.J., Hall, F.W., Tarantino, L.M., and Gekakis, N. 2005. Diabetes insipidus in mice with a mutation in aquaporin-2. *PLoS Genet.* **1**:e20.
27. Rojek, A., Füchtbauer, E.M., Kwon, T.H., Frøkiaer, J., and Nielsen, S. 2006. Severe urinary concentrating defect in renal collecting duct-selective AQP2 conditional-knockout mice. *Proc. Natl. Acad. Sci. U. S. A.* **103**:6037–6042.
28. Sohara, E., et al. 2006. Pathogenesis and treatment of autosomal-dominant nephrogenic diabetes insipidus caused by an aquaporin 2 mutation. *Proc. Natl. Acad. Sci. U. S. A.* **103**:14217–14222.
29. Shi, P.P., et al. 2007. Nephrogenic diabetes insipidus in mice caused by deleting COOH-terminal tail of aquaporin-2. *Am. J. Physiol. Renal Physiol.* **292**:F1334–F1344.
30. Brown, D., Katsura, T., and Gustafson, C.E. 1998. Cellular mechanisms of aquaporin trafficking. *Am. J. Physiol.* **275**:F328–F331.
31. Loonen, A.J., Knoers, N.V., van Os, C.H., and Deen, P.M. 2008. Aquaporin 2 mutations in nephrogenic diabetes insipidus. *Semin. Nephrol.* **28**:252–265.
32. Verkman, A.S. 2008. Dissecting the roles of aquaporins in renal pathophysiology using transgenic mice. *Semin. Nephrol.* **28**:217–226.
33. Uawithya, P., Pisitkun, T., Ruttenberg, B.E., and Knepper, M.A. 2008. Transcriptional profiling of native inner medullary collecting duct cells from

rat kidney. *Physiol. Genomics.* **32**:229–253.
34. Alexander, S.P., Mathie, A., and Peters, J.A. 2007. Guide to receptors and channels. *Br. J. Pharmacol.* **150**(Suppl. 1):S1–S168.
35. Purdy, K.E., and Arendshorst, W.J. 2000. EP_1 and EP_4 receptors mediate prostaglandin E_2 actions in the microcirculation of rat kidney. *Am. J. Physiol. Renal Physiol.* **279**:F755–F764.
36. Tang, L., Loutzenhiser, K., and Loutzenhiser, R. 2000. Biphasic actions of prostaglandin E_2 on the renal afferent arteriole: role of EP_3 and EP_4 receptors. *Circ. Res.* **86**:663–670.
37. Klussmann, E., Maric, K., and Rosenthal, W. 2000. The mechanisms of aquaporin control in the renal collecting duct. *Rev. Physiol. Biochem. Pharmacol.* **141**:33–95.
38. Hasler, U., et al. 2002. Long term regulation of aquaporin-2 expression in vasopressin-responsive renal collecting duct principal cells. *J. Biol. Chem.* **277**:10379–10386.
39. Bouley, R., Hasler, U., Lu, H.A., Nunes, P., and Brown, D. 2008. Bypassing vasopressin receptor signaling pathways in nephrogenic diabetes insipidus. *Semin. Nephrol.* **28**:266–278.
40. Hockel, G.M., and Cowley, A.W., Jr. 1979. Prostaglandin E_2-induced hypertension in conscious dogs. *Am. J. Physiol.* **237**:H449–H454.
41. Boone, M., and Deen, P.M. 2009. Congenital nephrogenic diabetes insipidus: what can we learn from mouse models? *Exp. Physiol.* **94**:186–190.
42. Pászty, C., et al. 1995. Lethal α-thalassaemia created by gene targeting in mice and its genetic rescue. *Nat. Genet.* **11**:33–39.
43. Deng, C., Wynshaw-Boris, A., Zhou, F., Kuo, A., and Leder, P. 1996. Fibroblast growth factor receptor 3 is a negative regulator of bone growth. *Cell.* **84**:911–921.
44. Xu, X., et al. 2001. Direct removal in the mouse of a floxed neo gene from a three-loxP conditional knockout allele by two novel approaches. *Genesis.* **30**:1–6.
45. Pisitkun, T., et al. 2008. Akt and ERK1/2 pathways are components of the vasopressin signaling network in rat native IMCD. *Am. J. Physiol. Renal Physiol.* **295**:F1030–F1043.
46. Chou, C.L., Rapko, S.I., and Knepper, M.A. 1998. Phosphoinositide signaling in rat inner medullary collecting duct. *Am. J. Physiol.* **274**:F564–F572.
47. Wall, S.M., Han, J.S., Chou, C.-L., and Knepper, M.A. 1992. Kinetics of urea and water permeability activation by vasopressin in rat terminal IMCD. *Am. J. Physiol.* **262**:F989–F998.
48. Qi, Z., et al. 2004. Serial determination of glomerular filtration rate in conscious mice using FITC-inulin clearance. *Am. J. Physiol. Renal Physiol.* **286**:F590–F596.
49. Faulhaber-Walter, R., et al. 2008. Lack of A1 adenosine receptors augments diabetic hyperfiltration and glomerular injury. *J. Am. Soc. Nephrol.* **19**:722–730.